Enhanced Efficiency of Metamorphic Triple Junction Solar Cells for Space Applications *

Du-Xiang Wang(王笃祥), Ming-Hui Song(宋明辉)**, Jing-Feng Bi(毕京锋), Wen-Jun Chen(陈文浚), Sen-Lin Li(李森林), Guan-Zhou Liu(刘冠洲), Ming-Yang Li(李明阳), Chao-Yu Wu(吴超瑜)

Tianjin San'an Optoelectronics Co., LTD., Tianjin 300384

(Received 7 February 2017)

Metamorphic $In_{0.55}Ga_{0.45}P/In_{0.06}Ga_{0.94}As/Ge$ triple-junction (3J-MM) solar cells are grown on Ge (100) substrates via metal organic chemical vapor deposition. Epi-structural analyses such as high resolution x-ray diffraction, photoluminence, cathodoluminescence and HRTEM are employed and the results show that the high crystal quality of 3J-MM solar cells is obtained with low threading dislocation density of graded buffer (an average value of $6.8\times10^4/cm^2$). Benefitting from the optimized bandgap combination, under one sun, AM0 spectrum, 25°C conditions, the conversion efficiency is achieved about 32%, 5% higher compared with the lattice-matched $In_{0.49}Ga_{0.51}P/In_{0.01}Ga_{0.99}As/Ge$ triple junction (3J-LM) solar cell. Under 1-MeV electron irradiation test, the degradation of the EQE and I–V characteristics of 3J-MM solar cells is at the same level as the 3J-LM solar cell. The end-of-life efficiency is ∼27.1%. Therefore, the metamorphic triple-junction solar cell may be a promising candidate for next-generation space multi-junction solar cells.

PACS: 88.40.hj, 88.40.jp, 84.60.Jt DOI: 10.1088/0256-307X/34/6/068801

Since InGaP/(In)GaAs/Ge space triple-junction solar cells have been used by Spectrolab corporation in the DIRECTV-4S satellite with the conversion efficiency of 24.5% in 2001,[1] multijunction solar cells in space applications have attracted considerable interest and have been developed dramatically. The state-of-the-art device structure is the $In_{0.49}Ga_{0.51}P/In_{0.01}Ga_{0.99}As/Ge$ triple junction solar cell, which is designed to be lattice matched since generation of misfit dislocations is minimized for higher photovoltaic conversion efficiency. After two decades of development, the conversion efficiency of the lattice-matched $In_{0.49}Ga_{0.51}P/In_{0.01}Ga_{0.99}As/Ge$ triple junction (3J-LM) solar cell is close to 30% under AM0, widely used for power production in space satellites.[2,3]

Meanwhile, theoretical calculations show that the band-gap combination of 3J-LM solar cells is not optimal in terms of efficiency optimization. By lowering the bandgap energies of top and middle subcells, higher efficiencies can be realistic with metamorphic structure solar cells, which have a more appropriate bandgap combination to convert the energy of the broad solar spectrum into electricity effectively.[4,5] Experimentally, under high concentration in terrestrial application, such metamorphic InGaP/InGaAs/Ge triple-junction solar cells were fabricated with 40.7% efficiency of $In_{0.56}Ga_{0.44}P/Ga_{0.92}In_{0.08}As/Ge$ cells and 42% of $In_{0.65}Ga_{0.35}P/Ga_{0.83}In_{0.17}As/Ge$ cells under 500 suns, AM1.5D, higher than 40% with 3J-LM solar cells.[6,7] Till now, under one sun in space application, only a few studies were reported on metamorphic structure solar cells worldwide. In this Letter, using optimized InGaAs graded buffer we obtain the metamorphic $In_{0.55}Ga_{0.45}P/In_{0.06}Ga_{0.94}As/Ge$ triple junction (3J-MM) solar cell with the band-gap combination of 1.88 eV/1.34 eV/0.67 eV. High efficiency of 32.0% is achieved with 30.15 cm^2 cell area at 25℃ under one sun, AM0. By 1-MeV electron irradiation testing, the cell performance degradation was also studied and an end-of-life efficiency ∼27.1% of the $In_{0.55}Ga_{0.45}P/In_{0.06}Ga_{0.94}As/Ge$ 3J-MM solar cell is obtained.

A production size AIX2800-G4 low-pressure metal organic chemical vapor deposition (LP-MOCVD) system was used for the growth of 3J-MM solar cells on 4 inch diameter (100)-oriented Ge substrates with 9° off-cut towards the [111] direction. The schematic structure of the 3J-MM solar cell is shown in Fig. 1. Trimethylindium (TMIn), trimethylgalium (TMGa), trimethylaluminum (TMAl), arsine (AsH_3), phosphine (PH_3), carbon tetrachloride (CCl_4), diethylzinc (DEZn) and diethyltellurium (DETe) were used as the MOCVD source materials, and H_2 was used as the carrier gas. The reactor pressure was maintained at 50 mbar with the growth temperature typically in the range of 600–700℃ during the growth.

After the growth, the epi-structure was analyzed by TEM and cathodoluminescence (CL) to reveal the misfit dislocation of epitaxial layers. High resolution x-ray diffraction (HRXRD) and photoluminence (PL) were used for characterizing the structural properties in terms of composition, crystal quality, strain, and relaxation.

Using a standard technology, the epi-structure was processed into 4×8 cm^2 chips with 2 cropped corners. The front grids were patterned by photolithography, and then the Ag/Au p-type and AuGe/Ni/Au/Ag n-type contact metals were deposited by e-beam evap-

*Supported by the Grand from Tianjin Little Giant Fund under Grant No 14ZXLJGX00400, and the Tianjin Science and Technology Support Plan under Grant No 16YFZCGX00030.

**Corresponding author. Email: songminghui_2007@163.com

© 2017 Chinese Physical Society and IOP Publishing Ltd

oration. The GaAs cap layer was selectively removed between the grid fingers using a citric acid/H_2O_2 mixture. Subsequently, an Al_2O_3/TiO_2 dual layer antireflection coating (ARC) was evaporated on the front surface of the cells to reduce incident light loss. The 30.15 cm^2 cell area was finally defined through a chemical etching.

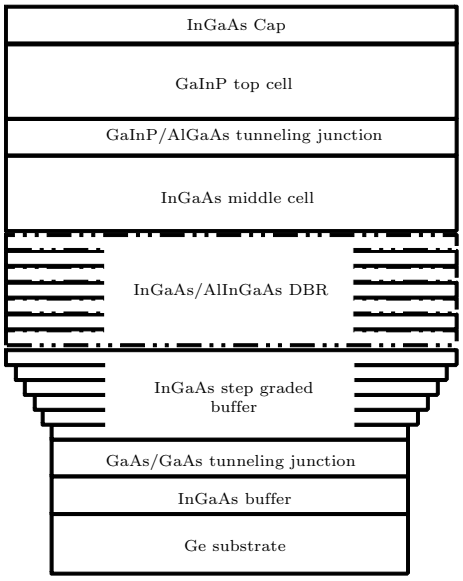

Fig. 1. Schematic structure of the 3J-MM solar cell.

Before and after 1-MeV electron irradiation testing, the external quantum efficiency (EQE) of 3J-MM solar cell was measured with a commercial Enlitech system, and the current–voltage (I–V) characteristics were also measured at 25℃ under AM0, 135.3 mW/cm^2, using a Spectrolab X-25 solar simulator, which was calibrated with isotype subcells of the 3J-MM solar cell.

In MOCVD reactors, InGaAs and InGaP epilayers are grown on a Ge substrate. Increasing the In content of the InGaAs or InGaP layers lowers the semiconductor bandgap energies, which also makes the ternary compound lattice mismatched with the Ge substrate, and leads to metamorphic growth condition. One of the most critical issues of metamorphic growth is the formation of misfit and threading dislocations, seriously influencing the performance of the 3J-MM solar cell as non-radiation recombination centers under one sun or low concentration conditions.[8–10] Metamorphic graded buffer is a mature method, used to reducing the upper influence. Proved by others' research, step graded buffer is more advantageous than linear graded buffer in terms of different growth schemes and InGaAs step graded buffer can easily show higher crystal quality than GaInP.[11,12]

In this study, using InGaAs step graded buffer we grow the $In_{0.55}Ga_{0.45}P/In_{0.06}Ga_{0.94}As/Ge$ 3J-MM solar cell, of which the band-gap combination of 1.88 eV/1.34 eV/0.67 eV is identified by PL and the lattice mismatch of 0.32% is identified by HRXRD between the top/middle cells and Ge substrate. Compared with that of the 3J-LM solar cell, a red shift of bandgap energies of InGaP top cell and InGaAs middle cell of the 3J-MM cell is observed in Fig. 2(a), which is consistent with the epi structure design. Meanwhile, high crystal quality of the 3J-MM solar cell was also demonstrated. From Fig. 2, the FWHM of PL is 12 meV of $In_{0.55}Ga_{0.45}P$ and 14 meV of $In_{0.06}Ga_{0.94}As$, respectively, and the (004)- and (224)-FWHM of the 3J-MM solar cell are 86 arcsec and 99 arcsec, respectively, close to ∼70 arcsec of $In_{0.49}Ga_{0.51}P/In_{0.01}Ga_{0.99}As/Ge$ 3J-LM solar cells. Figure 3 provides an asymmetric (224) glancing exit reciprocal space map (RSM), which indicates that the metamorphic graded buffer layer is 100% relaxed, and the main layers are lattice matched among the $In_{0.55}Ga_{0.45}P$ top cell, the $In_{0.06}Ga_{0.94}As$ middle cell and the $In_{0.06}Ga_{0.94}As$ target layer of graded buffer.

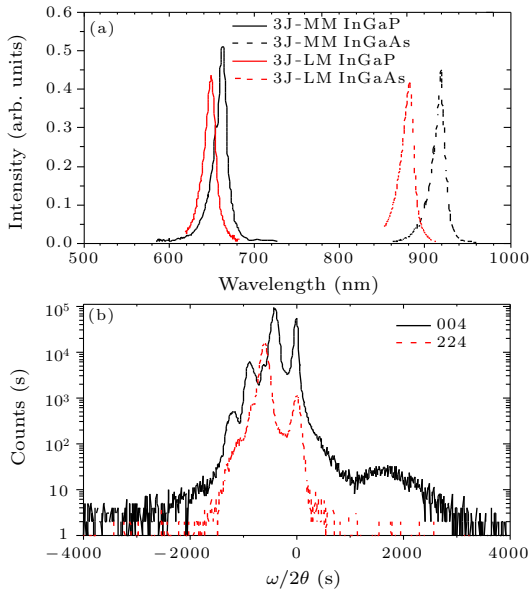

Fig. 2. PL spectrum of the InGaP top cell and the InGaAs middle cell of the 3J-MM solar cell, in comparison with that of the 3J-LM solar cell, and XRD rocking curves of (004) plane and (224) plane of the 3J-MM solar cell.

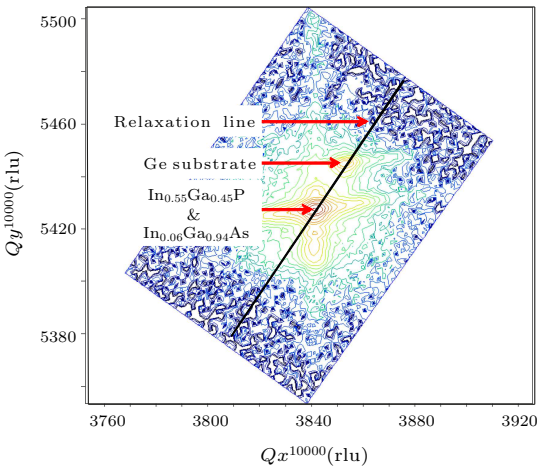

Fig. 3. XRD RSM of the 3J-MM solar cell using the asymmetric (224) glancing exit reflection.

To further check the crystal quality of the $In_{0.55}Ga_{0.45}P/In_{0.06}Ga_{0.94}As/Ge$ 3J-MM solar cell,

cross-sectional TEM is analyzed. From Fig. 4(a), all interfaces between adjacent layers are sharp, which are a critical element for solar cell efficiency. Figure 4(b) shows that the InGaAs step graded buffer consists of six layers with the total thickness of about 2 μm, and the thickness of each layer is around 300 nm, expecting the overshoot layer with 550 nm. The overshoot layer has higher In composition than the $In_{0.06}Ga_{0.94}As$ target layer, to balance the strain and prevent the spreading of the threading dislocations. Almost all of the dislocations are suppressed in the graded buffer. Only a small number of threading dislocations have penetrated the overshoot layer and have been figured out in the active layers, which is confirmed by the CL measurement. The graded buffer of three different locations along the 4-inch diameter epitaxial wafer (flat, center and round) was scanned via CL as shown in Fig. 5. It shows that the threading dislocation densities (TDDs) are counted to about $4.7 \times 10^4/cm^2$, $6.3\times10^4/cm^2$ and $9.4\times10^4/cm^2$, respectively, with the average value about $6.8\times10^4/cm^2$, which is lower than $\sim2.0 \times 10^5/cm^2$ of the $In_{0.08}GaAs$ layer in Ref. [9]. This very low TDD makes a contribution to the high efficiency, especially for large area solar cells to maximize the carrier mobility and to minimize the current leakage.

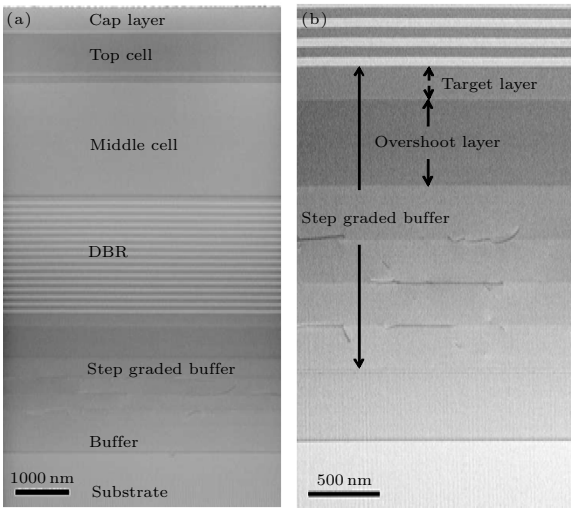

Fig. 4. TEM micrographs of (a) the whole epi-structure and (b) InGaAs step graded buffer of the 3J-MM solar cell.

Figure 6 indicates the EQE measurement of the $In_{0.55}Ga_{0.45}P/In_{0.06}Ga_{0.94}As/Ge$ 3J-MM solar cell, in comparison with that of the $In_{0.49}Ga_{0.51}P/In_{0.01}Ga_{0.99}As/Ge$ 3J-LM solar cell. Similar spectrum response intensities have been detected. The subcell current match condition is better in 3J-MM than the 3J-LM solar cell with the values of top cell, middle cell and bottom cell, 18.8 mA/cm^2, 19.7 mA/cm^2 and 22.8 mA/cm^2, respectively, as listed in Table 1. The current densities of top cell and middle cell of the 3J-MM solar cell are about 9% higher than that of the 3J-LM solar cell with a red shift of bandgap energies, while the current density is 16% lower for the bottom cell. This shift is consistent with the value from the PL spectrum in Fig. 2(a). The gap between the EQE curves of the $In_{0.06}Ga_{0.94}As$ middle cell and the Ge bottom cell results from the influence of DBR and the overshoot layer with higher indium content, while this gap in the case of the 3J-LM solar cell is only affected by DBR. Thus we can further improve the current density of the Ge bottom cell by changing the overshoot layer from InGaAs to AlInGaAs.

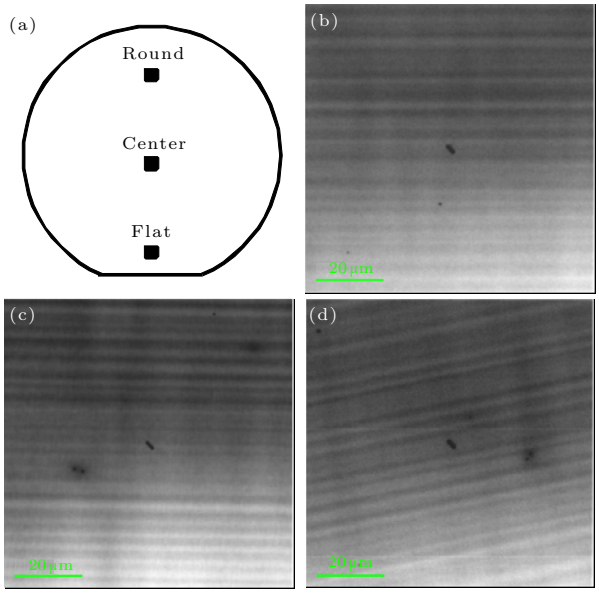

Fig. 5. CL images of graded buffer in (a) three different areas across the 4-inch diameter epitaxial wafer, (b) flat, (c) center and (d) round.

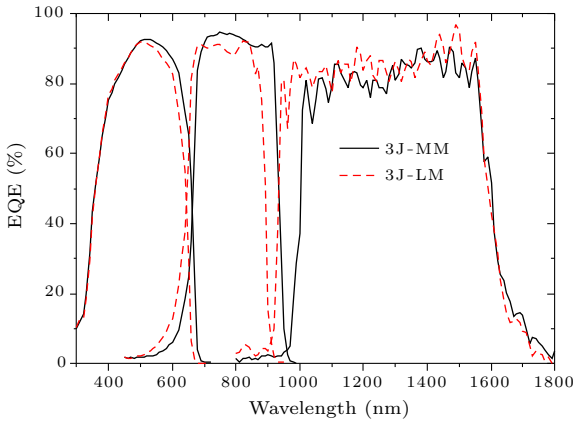

Fig. 6. EQE curves of the 3J-MM and 3J-LM solar cells.

From the I–V characteristics shown in Fig. 7, the high efficiency of 32.0% is achieved by the $In_{0.55}Ga_{0.45}P/In_{0.06}Ga_{0.94}As/Ge$ 3J-MM device structure, which illustrates the conception available under one sun. From Table 1 with cell area of 30.15 cm^2, the open circuit voltage (V_{oc}) of the 3J-MM solar cell is 80 mV lower, about 3% lower than that of the $In_{0.49}Ga_{0.51}P/In_{0.01}Ga_{0.99}As/Ge$ 3J-LM solar cell, while the short-circuit current I_{sc} is 50 mA higher, which is about 9% higher, and the fill factor (FF) is about 1% lower. Finally, the conversion efficiency (E_{ff}) obtains a 5% improvement compared with

the 3J-LM solar cell.

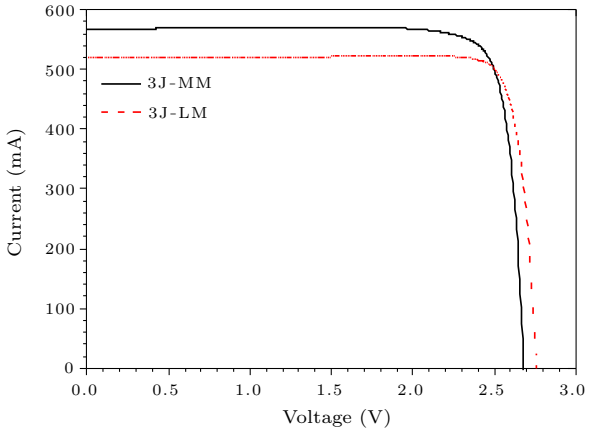

Fig. 7. The I–V curve of the 3J-MM solar cell under AM0 spectrum, 25℃, in comparison with that of the 3J-LM solar cell.

In the space environment, it is inevitable for solar cells to be radiated by high energy particles, such as protons and electrons, and the radiation hardness is a vital parameter for solar cells. Generally the cell performance degradation can be measured under 1-MeV electron irradiation with the fluence of 1×10^{15} e/cm^2. In Table 1, the cell characteristics are summarized for the $In_{0.55}Ga_{0.45}P/In_{0.06}Ga_{0.94}As/Ge$ 3J-MM solar cell before and after electron radiation. Compared with the $In_{0.49}Ga_{0.51}P/In_{0.01}Ga_{0.99}As/Ge$ 3J-LM solar cell, there is a similar degradation behavior. The EQE remaining factors (RFs) are 99% of the $In_{0.55}Ga_{0.45}P$ top cell, 93% of the $In_{0.06}Ga_{0.94}As$ middle cell and 95% of the Ge bottom cell, respectively, which are similar to that of the 3J-LM solar cell. Thus the InGaP top cell has the superior radiation hardness, and radiation damage of the InGaAs middle cell is most serious, which results in a transition of the current-limited cell from the top to the middle cell, while the Ge bottom cell shows less radiation degradation than the middle cell and still the highest current density because of the wide spectrum response range. Similar results have also been reported in Ref. [13]. Meanwhile, the RFs of I_{sc} and FF are 98% and 98%, respectively, also similar to the 3J-LM solar cell, while 88% of V_{oc} and 84.6% of E_{ff} are slightly lower than 89% and 85.4% of the 3J-LM solar cell, respectively. Finally, the end-of-life efficiency ∼27.1% of the $In_{0.55}Ga_{0.45}P/In_{0.06}Ga_{0.94}As/Ge$ 3J-MM solar cell is obtained after electron radiation, 4% relatively higher than 26.0% of the $In_{0.49}Ga_{0.51}P/In_{0.01}Ga_{0.99}As/Ge$ 3J-LM solar cell.

Table 1. EQE and I–V characteristics of the 3J-MM solar cell before and after 1-MeV electron radiation, compared with the 3J-LM solar cell.

Cell structure	Fluence (e/cm^2)	EQE_top (mA/cm)^2)	EQE_mid (mA/cm^2)	EQE_bot (mA/cm^2)	V_{oc} (V)	I_{sc} (mA)	FF (%)	E_{ff} (%)
		18.8	19.7	22.8	2.67	570	86	32.0
3J_MM	1×10^{15}	18.6	18.4	21.5	2.36	558	84	27.1
	RF	99%	93%	95%	88%	98%	98	84.6
		17.2	18.0	26.9	2.75	520	87	30.5
3J-LM	1×10^{15}	17.0	16.8	25.7	2.46	508	85	26.0
	RF	99%	93%	96%	89%	98%	98	85.4

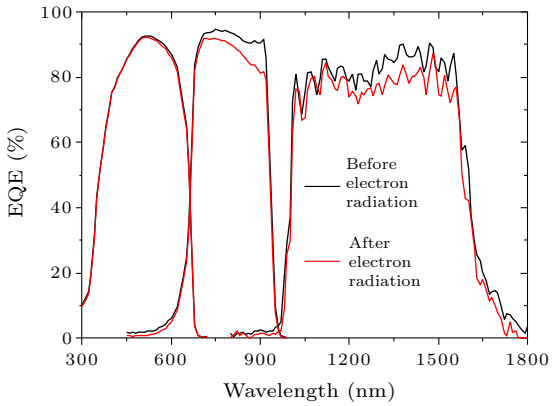

Fig. 8. EQE curves of the 3J-MM solar cell before and after electron radiation.

As we all know, induced by high energy particle radiation the defects can result in the decrease of minority-carrier diffusion length and lifetime and free carrier concentration and the increase of interface recombination velocity as recombination centers, which reduce the photo-generated carrier collection efficiency and increase the junction dark current, and therefore degrade the cell performance. For I–V parameters, the I_{sc} degradation can be explained by the EQE degradation of the subcells. Compared with the 3J-LM solar cell, the similar EQE_Top/EQE_Mid ratio before electron irradiation and the similar EQE RFs of the subcells after electron irradiation lead to the similar RF of I_{sc} of the 3J-MM solar cell. Moreover, the V_{oc} degradation is due to the increase of the junction dark current and the decrease of the parallel resistance.[15] The TDD of the 3J-MM solar cell is about 6.8×10^4/cm^2, which is higher than $\sim1\times10^4$/cm^2 of the 3J-LM solar cell, and the more threading dislocations could lead to the more degradation of junction dark current and parallel resistance and the more degradation of V_{oc} under electron radiation. Figure 8 shows the EQE curves before and after electron radiation of the $In_{0.55}Ga_{0.45}P/In_{0.06}Ga_{0.94}As/Ge$ 3J-MM solar cell. Based on the theory in Ref. [14], for the $In_{0.55}Ga_{0.45}P$ top cell and $In_{0.06}Ga_{0.94}As$ middle cell the spectral response degradation is observed mainly from long wavelength, which is induced by the decrease of the minority carrier diffusion length, while

the decline of almost the whole EQE curve of the Ge bottom cell is mainly due to the decrease of the free carrier concentration, which causes the deterioration of built-in potential. More investigations need to be carried out to further demonstrate the radiation hardness of the 3J-MM solar cell.

In summary, we have grown an $In_{0.55}Ga_{0.45}P/In_{0.06}Ga_{0.94}As/Ge$ 3J-MM solar cell on a 9°-off Ge (100)-oriented substrate in an LP-MOVPE system. HRXRD, PL, TEM and CL analyses indicate a good crystal quality of the 3J-MM solar cell. In comparison with the 3J-LM solar cell, the subcell current match is optimized and the short-circuit current of triple junction is increased by 9% with the open-circuit voltage reduced by 3%. The final efficiency of 32.0% is achieved under AM0, 5% higher than that of the 3J-LM solar cell. Under 1-MeV electron irradiation test, it is observed that remaining factors of the most characteristics of the 3J-MM solar cell are similar to that of the 3J-LM solar cell, and the end-of-life efficiency of the $In_{0.55}Ga_{0.45}P/In_{0.06}Ga_{0.94}As/Ge$ 3J-MM solar cell is shown to be 27.1%. Thus the metamorphic triple-junction solar cell seems to be a very promising path to increasing the efficiency of multi-junction solar cells for space application in the near future.

We acknowledge the Shanghai Institute of Space Power-Sources for the solar cell testing and the Xinjiang Technical Institute of Physics and Chemistry, Chinese Academy of Sciences for the electron irradiation testing.

References

[1] http://boeing.mediaroom.com/2001-11-26-Successful-Launch-Sends-Boeing-Built-DIRECTV-4S-Satellite-to-Orbit
[2] King R R et al 2002 *Proc. 29th IEEE Photovoltaic Specialists Conference* p 776
[3] Strobl G F X et al 2012 *Proc. 27th European Photovoltaic Solar Energy Conference and Exhibition* p 104
[4] Kurtz S R et al 2002 *Appl. Phys. Lett.* **80** 1379
[5] Zhang H et al 2010 *Sci. Chin. Technol. Sci.* **53** 2569
[6] King R R, Law D C, Edmondson K M, Fetzer C M, Kinsey G S, Yoon H, Sherif R A and Karam N H 2007 *Appl. Phys. Lett.* **90** 183516
[7] Fuhrmann D, Meusel M, Ebel L, Guter W, Kubera T, Köstler W and Strobl G 2013 *Proc. 9th International Conference on Concentrator Photovoltaic Systems* p 1
[8] King R R, Law D C, Edmondson K M, Fetzer C M, Kinsey G S, Yoon H, Krut D D, Ermer J H, Sherif R A and Karam N H 2007 *Adv. OptoElectron.* **2007** 29523
[9] Fetzer C M, King R R, Colter P C, Edmondson K M, Law D C, Stavrides A P, Yoon H, Ermer J H, Romero M J and Karam N H 2004 *J. Cryst. Growth* **261** 341
[10] Dimroth F, Schubert U and Bett A W 2000 *IEEE Electron Device Lett.* **21** 209
[11] Bett A W, Baur C, Dimroth F and Schöne J 2005 *Mater. Res. Soc. Symp. Proc.* **836** L6.4
[12] King R R, Haddad M, Isshiki T, Colter P, Ermer J, Yoon H, Joslin D E and Karam N H 2000 *Proc. 28th IEEE Photovoltaic Specialists Conference* p 982
[13] Meusel M, Baur C, Guter W, Hernle M and Dimroth F 2005 *Proc. 20th European Photovoltaic Solar Energy Conference and Exhibition* p 20
[14] Walters R J, Messenger S R, Cotal H R, Xapsos M A, Wojtczuk S J, Serreze H B and Summers G P 1997 *J. Appl. Phys.* **82** 2164
[15] Hu J M, Wu Y Y, Qian Y, Yang D Z and He S Y 2009 *Acta Phys. Sin.* **58** 5051 (in Chinese)